

Nanoparticles-enabled low temperature growth of carbon nanofibers and their properties for supercapacitors

Rickard Andersson^{1*}, Amin M. Saleem¹, Ioanna Savva², Theodora Krasia-Christoforou², Peter Enoksson³, Vincent Desmaris¹

¹Smoltek AB, Regnbågsgatan 3, Gothenburg, SE-41755, Sweden

²Department of Mechanical and Manufacturing Engineering, University of Cyprus, Nicosia, Cyprus

³Microtechnology and Nanoscience, Electronics Materials and Systems Laboratory, Chalmers University of Technology, Gothenburg, SE-41296, Sweden

DOI: 10.5185/amlett.2018.1948

www.vbripress.com/aml

Abstract

Carbon nanostructures are of great interest for a variety of applications, but their current processing throughput limits their industrial full scale deployment. This paper presents a cost effective and simple fabrication process, where vertically aligned carbon nanofibers are grown using DC-PECVD at CMOS compatible temperatures from catalytic nanoparticles, spin-coated from stable polymer-nanoparticle colloidal suspensions. Two different catalysts, Co and Cu, are investigated by growing carbon nanofibers at temperatures ranging from 390 °C to 550 °C, using suspensions with various concentrations of nanoparticles. The length and morphology of the grown nanofibers are examined using SEM and the electrical properties are investigated using electrochemical measurements on samples arranged as supercapacitor devices. Vertically aligned CNFs are successfully grown from both types of catalyst. The Co-derived fibers are long and arranged in a denser carpet-like structure, while the Cu-derived fibers are shorter and in a sparser formation of free-standing individual fibers. All electrochemical measurements show typical supercapacitor behaviour even at high scan rates of 200 mVs⁻¹, with the fibers grown from Co showing great increase in capacitance over the bare chip reference device, including the samples grown at 390 °C. Copyright © 2018 VBRI Press.

Keywords: Nanoparticles, carbon, nanofibers, CNF, supercapacitor

Introduction

Carbon nanostructures are extensively researched for different applications in the microelectronics and semiconductor packaging industry, due to the natural abundance of carbon, along with extraordinary properties such as high thermal conductivity, good mechanical strength, and excellent electrical conductivity. For example, their electrical and mechanical properties make them interesting for interconnect applications, and the thermal properties of carbon nanostructures can be used for heat dissipation and heat transportation [1]. Furthermore, their high surface area to volume ratio makes carbon nanostructures a widely studied candidate for electrode materials in different capacitor applications, such as the electrical double layer capacitors (EDLCs) commonly referred to as supercapacitors [1-12].

In order to avoid expensive and time consuming transfer processing steps however, the nanostructures should be grown directly at the desired location on the

substrate using a deposited catalyst to control the growth. Doing so creates a number of challenges, such as keeping the growth temperature low enough to leave the substrate and any other components present unharmed, and keeping the catalyst deposition process simple, thus ensuring high throughput.

One carbon nanostructure suitable for controlled growth at a desired location is the carbon nanofiber (CNF), consisting of cone shaped graphene sheets stacked inside each other to form a solid fiber [1]. CNFs have been proven to grow at temperatures below 400 °C, thus making the process temperature CMOS compatible, in a controlled pattern that is defined by for example a liftoff process [13-14]. CNFs have also been investigated in supercapacitor applications, grown either as a film such as for an electrode in a coin-cell device [6], or grown in a patterned structure to form interdigitated solid state gel electrolyte based supercapacitors [15].

In this work we compare the length, morphology, and electrical performance of vertically aligned carbon nanofibers (VACNFs) grown at CMOS compatible temperatures ($< 400\text{ }^{\circ}\text{C}$), using colloidal suspensions of different polymer-stabilized nanoparticles (NPs) as the catalyst source for the CNF growth by means of direct current plasma enhanced chemical vapour deposition, DC-PECVD. The nanoparticle suspensions are simply spin-coated onto the samples [16], without the need for complicated and expensive equipment or processing for the catalyst deposition. Further advantages of using these catalytical colloidal suspensions are their non-toxicity and their low cost.

Experimental

Chemical reagents

Polyvinylpyrrolidone (PVP, 1300000 g/mol), copper(II) acetate monohydrate ($(\text{CO}_2\text{CH}_3)_2\text{Cu}\cdot\text{H}_2\text{O}$, 98%) hydrazine monohydrate (98%) and cobalt acetate ($(\text{CH}_3\text{CO}_2)_2\text{Co}$, 99.995%) were purchased from Sigma-Aldrich. Methanol (analytical grade, ACS reagent) was purchased from Scharlau. The above-mentioned reagents were used as provided by the manufacturer without further purification.

Synthesis of PVP-stabilized Cu nanoparticles

The PVP/Cu colloidal solution (mols vinyl pyrrolidone (VP) units/mols $(\text{CO}_2\text{CH}_3)_2\text{Cu}\cdot\text{H}_2\text{O} = 300:1$) were prepared as follows: In a vial equipped with a magnetic stirrer, PVP (2.0 g, 18 mmol of VP units) was dissolved in MeOH (20 mL). Subsequently, $(\text{CO}_2\text{CH}_3)_2\text{Cu}\cdot\text{H}_2\text{O}$ (11.8 mg, 0.06 mmol) was added to the polymer solution and the mixture was left to stir under inert atmosphere (N_2) for 30 minutes at room temperature until all components were completely dissolved. Afterwards, hydrazine monohydrate (14.7 μL , 0.3 mmol) was added and the colour of the solution became dark red/brown, indicating the formation of Cu NPs. The above-mentioned procedure was followed for the preparation of 2 more PVP/Cu systems with different Cu NP loading by varying the quantities of the reagents, as seen in **Table 1**.

Table 1. Quantities of the reagents used for the different PVP/Cu systems.

Sample code	PVP (mmol)	MeOH (mL)	Cu(II) salt (mmol)	Hydrazine (mmol)
300:1	18	20	0.060	0.3
150:1	18	20	0.120	0.6
75:1	18	20	0.240	1.2

Synthesis of PVP/Co hybrid solution

The PVP/Co(II) solutions (mols (VP) units/mols $(\text{CH}_3\text{CO}_2)_2\text{Co} = 300:1$) were prepared as follows: In a round bottom flask equipped with a magnetic stirrer, PVP (2.0 g, 18 mmol of VP units) was dissolved in MeOH (20 mL). Subsequently, $(\text{CH}_3\text{CO}_2)_2\text{Co}$ (10.6 mg, 0.06 mmol) was added to the polymer solution and the reaction mixture was left to stir for 2 hours at room temperature until all components completely dissolved. The above-mentioned procedure was followed for the preparation of 2 more PVP/Co(II) systems with different Co(II) loading, by varying the quantities of the reagents, as seen in **Table 2**.

Table 2: Quantities of the reagents used for the different PVP/Co systems

Sample code	PVP (mmol)	MeOH (mL)	$(\text{CH}_3\text{CO}_2)_2\text{Co}$ (mmol)
300:1	18	20	0.06
150:1	18	20	0.12
75:1	18	20	0.24

Sample fabrication

An oxidized Si wafer was diced into square 14 mm by 14 mm samples. A metal stack of Ti/TiN was sputtered on each side of the individual samples to ensure a good electrical ohmic contact between the front and back since backside probing would be used during the electrochemical characterization.

The different colloidal solutions were spin-coated onto the samples using a standard resist spinner, followed by baking on a hotplate. VACNFs were then grown through DC-PECVD using a mixture of ammonia and acetylene as process gasses for 2 h at different temperatures. Before letting the gasses into the chamber the samples underwent a heating step in vacuum to remove the polymer through thermal decomposition, thus leaving the NPs deposited on the sample surface [18]. Each growth run contained two identical samples, forming the two electrodes of an EDLC in the ensuing electrochemical analysis setup. The samples coated with a PVP/Co(II) solution were also subjected to an in situ annealing step for 2 h at $325\text{ }^{\circ}\text{C}$ in an N_2 environment in order for the Co(II) to form Co NPs. [17]

Two samples were also left without any CNF growth, i.e. only the TiN surface, to serve as reference.

Materials characterizations

The CNF length and fill-factor was characterized using a scanning electron microscope (SEM), taking images at normal incidence to the sample as well as at 40° tilt.

Cyclic voltammetry measurements were performed in a two electrode setup mimicking a supercapacitor device, where two identical CNF covered samples formed the two electrodes. Measurements were carried out using different scan rates ranging from 5 mVs^{-1} to 200 mVs^{-1} . The electrolyte used was 1 M KOH.

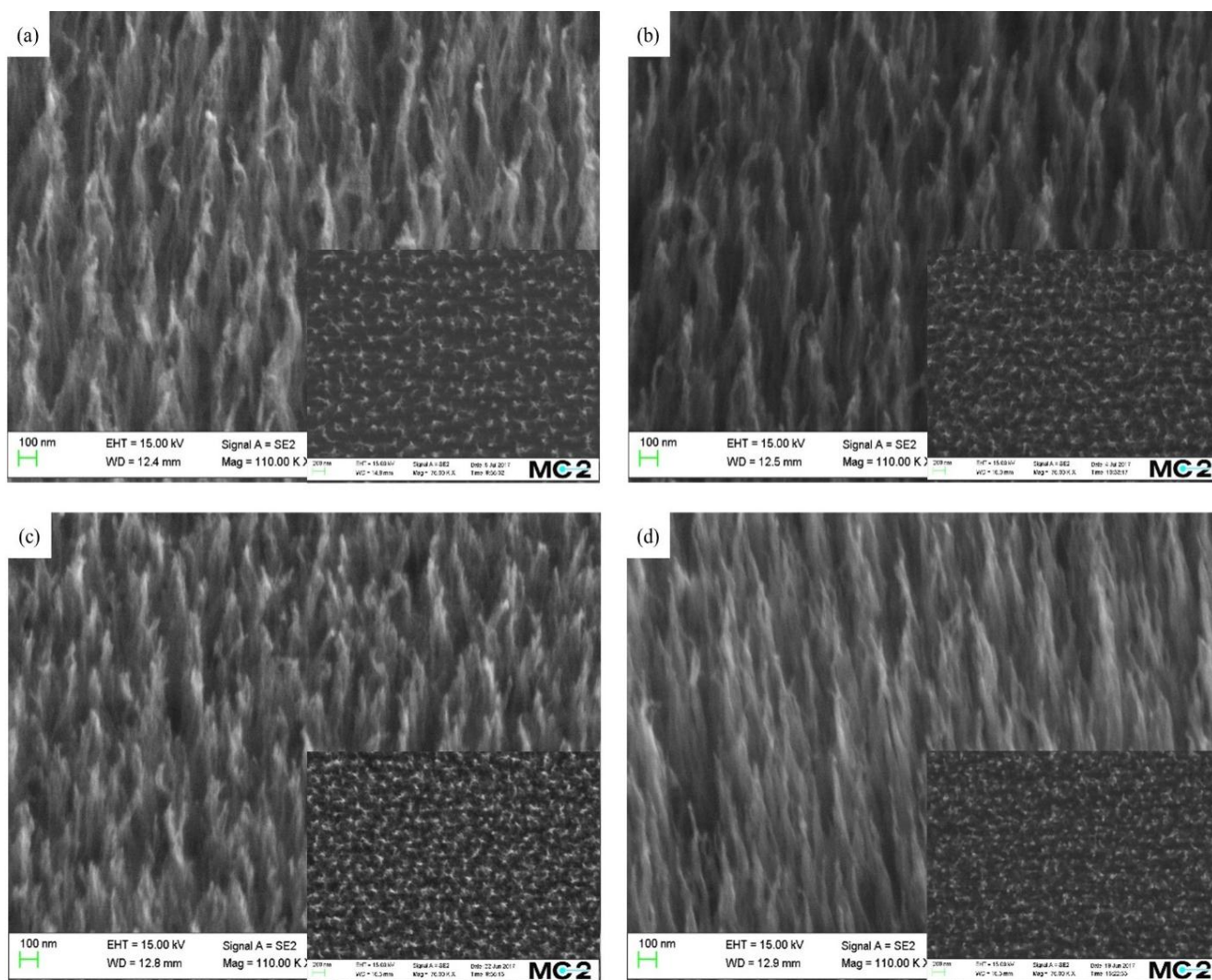


Fig. 1. SEM images taken at 40 ° tilt and 0 ° tilt (insets) of CNFs grown from (a) PVP/Co (300:1) at 390 °C. (b) PVP/Co (150:1) at 390 °C. (c) PVP/Co (75:1) at 390 °C. (d) PVP/Co (75:1) at 550 °C.

Results and discussion

Fig. 1(a) - (c) shows SEM images of the CNFs grown from the different PVP/Co systems at 390 °C both from a tilted view and from along the fiber axis (insets), while **Fig. 1(d)** shows the growth resulting from PVP/Co (75:1) at 550 °C. Similarly, **Fig. 2(a) – (c)** shows CNFs grown at 550 °C from the different PVP/Cu systems, while **Fig. 2(d)** shows the CNFs grown from PVP/Cu (75:1) at 390 °C. The different NP catalyst solutions yield CNFs with different length and fill-factors. The scale bars on the tilted images are the same for the two figures. **Fig. 3** illustrates the measured length of the CNFs grown from different solutions.

As shown in **Fig. 1** all fibers grown from the PVP/Co solutions are vertically aligned, and the images taken at zero tilt clearly demonstrate that a lowering of cobalt concentration leads to a lower CNF fill-factor when subjected to an identical growth environment. The top view images also illustrate the uniformity of the CNF film after spin-coating the samples, which is in line with

previously published results for CNFs grown by spin-coating PVP/Pd solutions [16].

The length of the PVP/Co grown fibers increases with the growth temperature (**Fig. 3**), as suggested by [17]. This becomes most evident by studying the PVP/Co (75:1) solution.

The CNFs grown from the PVP/Cu solutions display a very different morphology compared to the PVP/Co ones. As seen in **Fig. 2** they are much sparser and grow as individual free-standing fibers rather than as a CNF carpet. The NP concentration also has a dramatic impact on the fiber fill-factor as seen by comparing the insets of **Fig. 2(a) – (c)**, the first of which showing fibers only growing in clusters around larger particles that are spread out over the sample.

Fig. 2(d) also shows that there is little to no CNF growth from the copper NPs at 390 °C, indicating either that 390 °C is not a suitable temperature for CNF growth using Cu as catalyst, or that altering the growth parameters is required.

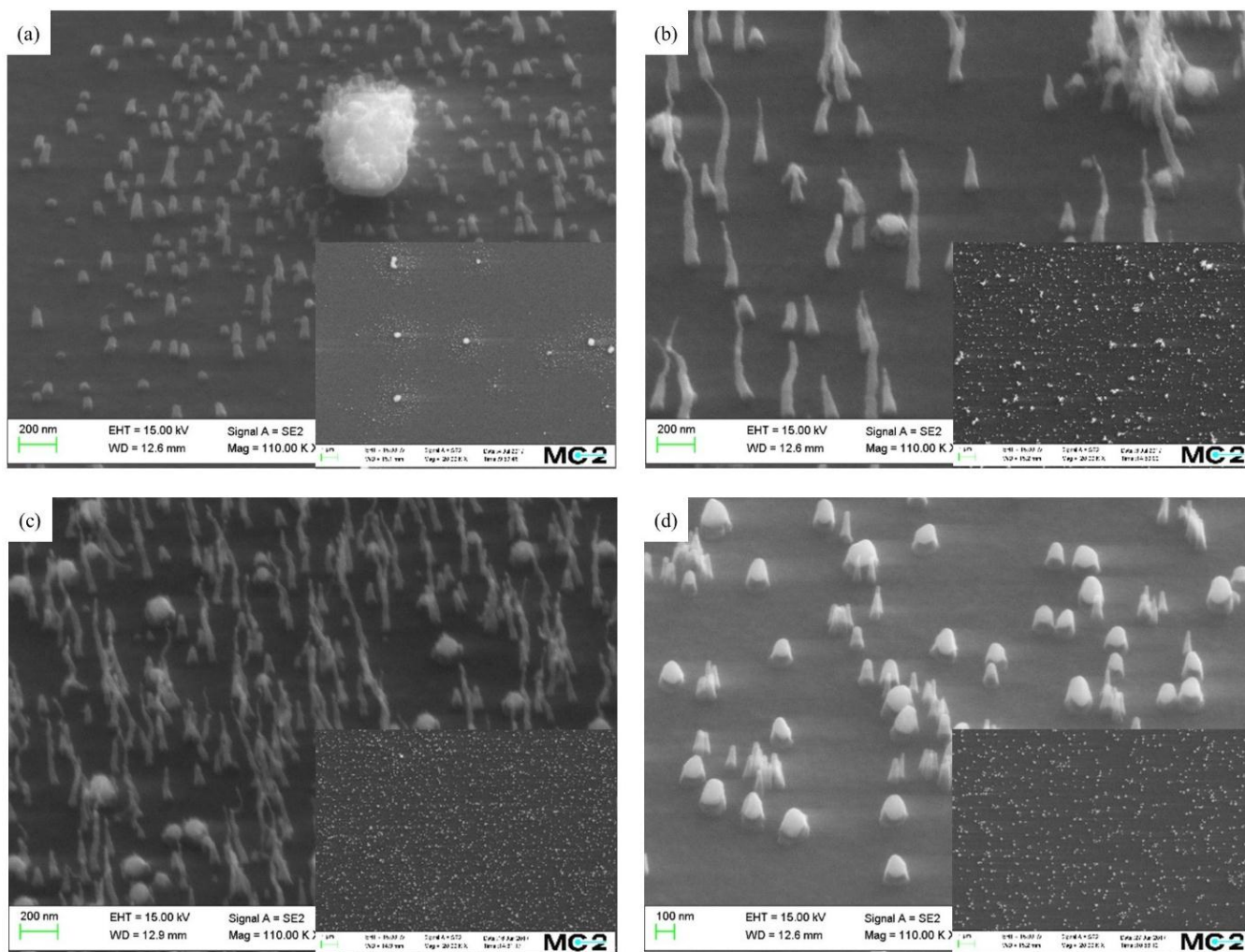


Fig. 2. SEM images taken at 40° tilt and 0° tilt (insets) of CNFs grown from (a) PVP/Cu (300:1) at 550 °C. (b) PVP/Cu (150:1) at 550 °C. (c) PVP/Cu (75:1) at 550 °C. (d) PVP/Cu (75:1) at 390 °C.

The results of the electrochemical analysis are provided in **Fig. 4**, showing the CV curves at different scan rates for one device (PVP/Co (75:1) at 550 °C) in **Fig. 4(a)**, and the capacitance per footprint area for all devices in **Fig. 4(b)**. The near rectangular shape of the CV curves demonstrates the electrical double layer capacitor behavior of the grown CNFs, while the slight peaks at the ends indicate an influence of a pseudocapacitive charge storage. It is known that carbon EDLCs display part of their capacitance as pseudocapacitance caused by the Faradaic reactivity of surface oxygen-functionalities, which should be abundant along the edges of the cone shaped graphene layers that stack to form a CNF [20].

Another significant characteristic for electrode materials is the rate stability, which is demonstrated by the good shape retention of the CV curves even as the scan rate is increased to 200 mVs⁻¹.

From **Fig. 4(b)** it is evident that the capacitance for the CNFs grown from the PVP/Cu systems is approximately the same as for the bare-chip reference device. The implication is that the resulting CNFs are not long enough, and the CNF film is not dense enough, to create a 3D structure with a significant impact on the

available surface area of the electrodes. An increase in capacitance for the PVP/Cu-grown CNF electrodes should follow if the parameters for the NP suspension and the growth are optimized to ensure longer fibers in a denser film.

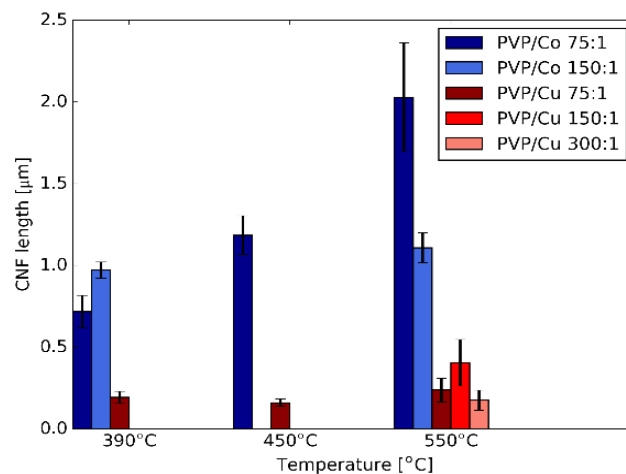


Fig. 3. The measured CNF length for different solutions at different growth temperatures.

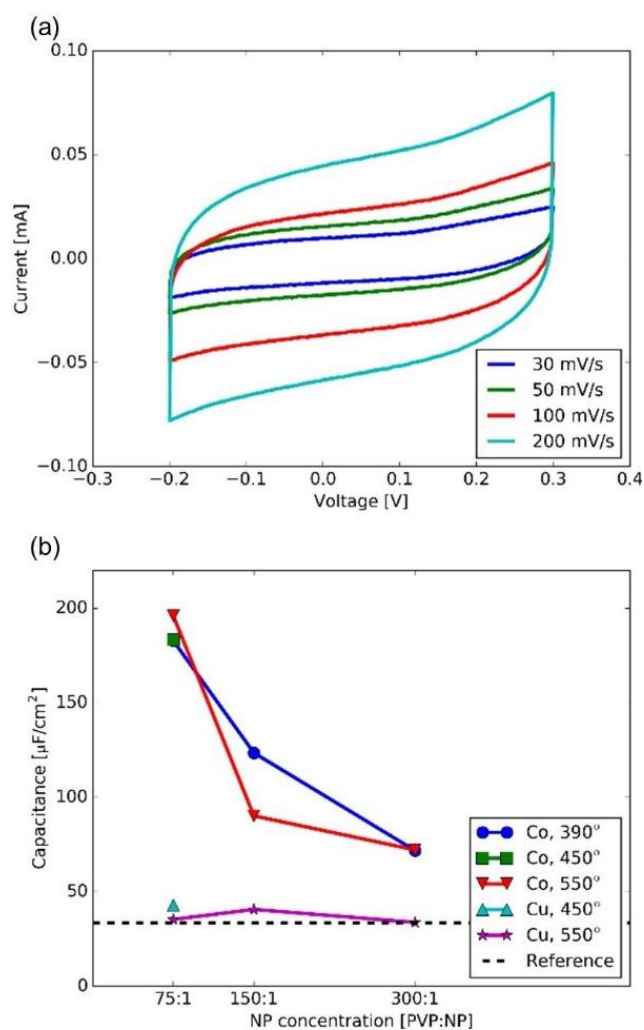


Fig. 4. (a) The CV curves from the PVP/Co (75:1) sample grown at 550 °C at different scan rates. (b) The measured capacitance per footprint area for the samples from different solutions at different growth temperatures.

The supercapacitor devices derived from the PVP/Co catalysts, however, show significant improvement over the reference, as expected since the CNF structures are both longer and denser for these samples. The fill-factor of the CNF film seems to bear more significance to the capacitance, and by extension the available surface area, than the fiber length, as evidenced in **Fig. 4 (b)**; the capacitance values for the CNFs grown at 390 °C using the Co-based samples drop significantly as the concentration of the NPs is lowered, even though it is seen in **Fig. 3** that the fibers are longer for the PVP/Co (150:1) solution than for PVP/Co (75:1) at 390 °C.

Previously published studies of PVP/Pd catalytic suspensions also indicate that the fill-factor of the CNFs has the most significant impact on the capacitance, and that it can be controlled by changing the NP concentration [16]. In that case the specific capacitances per footprint area at 100 mVs^{-1} scan rate were found to be 0.6 mFcm^{-2} and 1.2 mFcm^{-2} for PVP/Pd (38:1) and PVP/Pd (18:1) respectively, which in combination with the results from

this study further supports the claim that an increased NP loading leads to an increased capacitance.

The capacitance seems however to decrease with increasing CNF growth temperature for some devices. Since an increase in growth temperature results in longer CNFs (**Fig. 3**), the effect should be an increased surface area of the electrode, and thus an increase in capacitance, as seen for the PVP/Co (75:1) solution and in previous work [17]. One explanation for this could be an incomplete thermal decomposition of the PVP. The thermal decomposition of pure PVP starts at ca 380 °C [19], meaning that 390 °C is close to the limit where this occurs. It is possible that the heat pretreatments done at lower temperature growths did not fully remove all of the polymer, thus leaving residues that could possibly have reacted under the growth conditions to form a carbonaceous structure contributing to the capacitance via an increase in surface area compared to samples undergoing complete PVP burn-off. As seen in **Fig. 3** the fiber length increases more dramatically for the PVP/Co (75:1) solution when the growth temperature is increased compared to the other NP concentrations. The large increase in surface area for this concentration of NPs due to fiber length could then be enough to negate the impact of PVP residues at lower temperatures. Another explanation is the tendency for the CNFs to bundle together as they grow longer to form straighter CNF pillars. This is somewhat visible in **Fig. 1(d)**. The shorter CNFs (**Fig. 1(a) – (c)**) form a more porous structure of thinner, curlier, CNF strands. Thus, it can be the case that less surface area is available to the electrolyte for the higher temperature growths even though the fibers are longer, simply because a smaller percentage of each individual fiber is available to the electrolyte when they bundle together.

Conclusion

We successfully demonstrated a fast, simple, and cost effective method for growing vertically aligned CNFs at CMOS compatible temperatures by spin-coating different PVP-NP colloidal suspensions containing Cu or Co NPs. VACNFs were then grown from these nano-catalyst-particles using DC-PECVD at temperatures ranging from the CMOS compatible 390 °C up to 550 °C. SEM analysis has proven that the fill-factor of the CNF film can be controlled through the concentration of NPs in the suspension, and it is further shown through electrochemical measurements that the CNF films exhibit capacitive behavior typical for the electric double layer, making them feasible as electrode materials in a supercapacitor. Additionally, it is demonstrated that the fill-factor is of higher importance than fiber length for the capacitance in a supercapacitor application.

Acknowledgements

This work was supported by the grant “Postdoctoral Researchers” of the University of Cyprus supporting Dr. Ioanna Savva.

Author's contributions

Authors have no competing financial interests.

References

1. Desmaris, V.; Saleem, A. M.; Shafiee, S.; *IEEE Nanotechnology Magazine*, **2015**, 9, 33
DOI: [10.1109/MNANO.2015.2409394](https://doi.org/10.1109/MNANO.2015.2409394)
2. Kim, M. S.; Hsia, B.; Carraro, C.; Maboudian, R.; *Carbon*, **2014**, 74, 163
DOI: [10.1016/j.carbon.2014.03.019](https://doi.org/10.1016/j.carbon.2014.03.019)
3. Huang, P. et al.; *Science*, **2016**, 351, 691
DOI: [10.1126/science.aad3345](https://doi.org/10.1126/science.aad3345)
4. Lai, F.; Miao, Y.-E.; Zuo, L.; Lu, H.; Huang, Y.; Liu, T.; *Small*, **2016**, 12, 3235
DOI: [10.1002/sml.201600412](https://doi.org/10.1002/sml.201600412)
5. Yu, J. et al.; *ACS Nano*, **2016**, 10, 5204
DOI: [10.1021/acsnano.6b00752](https://doi.org/10.1021/acsnano.6b00752)
6. Saleem, A. M.; Boschini, A.; Lim, D.-H.; Desmaris, V.; Johansson, P.; Enoksson, P.; *Int. J. Electrochem. Sci.*, **2017**, 12, 6653
DOI: [10.20964/2017.07.46](https://doi.org/10.20964/2017.07.46)
7. Saleem, A.M.; Desmaris, V.; Enoksson, P.; *J. Nanomater.*, **2016**, 2016, 17
DOI: [10.1155/2016/1537269](https://doi.org/10.1155/2016/1537269)
8. Jian, L. et al.; *Nano Lett.*, **2013**, 13, 72
DOI: [10.1021/nl3034976](https://doi.org/10.1021/nl3034976)
9. El-Kady, M. F.; Strong, V.; Dubin, S.; Kaner, R. B.; *Science*, **2012**, 335, 1326
DOI: [10.1126/science.1216744](https://doi.org/10.1126/science.1216744)
10. Hsia, B. et al.; *Nanotechnology*, **2014**, 25, 055401
DOI: [10.1088/0957-4484/25/5/055401](https://doi.org/10.1088/0957-4484/25/5/055401)
11. Peng, Z.; Lin, J.; Ye, R.; Samuel, E. L. G.; Tour, J. M.; *ACS Appl. Mater. Interfaces*, **2015**, 7, 3414
DOI: [10.1021/am509065d](https://doi.org/10.1021/am509065d)
12. Beidaghi, M.; Gogotsi, Y.; *Energy Environ. Sci.*, **2014**, 7, 867
DOI: [10.1039/C3EE43526A](https://doi.org/10.1039/C3EE43526A)
13. Desmaris, V.; Saleem, A.; Shafiee, S.; Berg, J.; Kabir, M.; Johansson, A.; Marcoux, P.; IEEE Electron. Compon. Technol. Conf., Proc. 64, Orlando, FL, USA, Vol. 64, **2014**, pp. 1071-1076
DOI: [10.1109/ECTC.2014.6897421](https://doi.org/10.1109/ECTC.2014.6897421)
14. Saleem, A. M.; Berg, J.; Desmaris, V.; Kabir, M.; *Nanotechnology*, **2009**, 20, 375302
DOI: [10.1088/0957-4484/20/37/375302](https://doi.org/10.1088/0957-4484/20/37/375302)
15. Saleem, A. M.; Andersson, R.; Desmaris, V.; Song, B.; Wong, C. P. Session 4: Advanced Substrates and Integrated Devices, IEEE Electron. Compon. Technol. Conf., Proc. 67, Orlando, FL, USA, Vol. 67, **2017**, pp. 173 - 178
DOI: [10.1109/ECTC.2017.135](https://doi.org/10.1109/ECTC.2017.135)
16. Saleem, A. M.; Shafiee, S.; Krasia-Christoforou, T.; Savva, I.; Göransson, G.; Desmaris, V.; Enoksson, P.; *Sci. Technol. Adv. Mater.*, **2015**, 16, 015007
DOI: [10.1088/1468-6996/16/1/015007](https://doi.org/10.1088/1468-6996/16/1/015007)
17. Saleem, A. M.; Göransson, G.; Desmaris, V.; Enoksson, P.; *Solid-State Electron.*, **2015**, 107, 15
DOI: [10.1016/j.sse.2015.01.022](https://doi.org/10.1016/j.sse.2015.01.022)
18. Shao, H.; Huang, Y.; Lee, H.S.; Suh, Y. J.; Kim, C. O.; *Current Applied Physics*, **2006**, 6, e195
DOI: [10.1016/j.cap.2006.01.038](https://doi.org/10.1016/j.cap.2006.01.038)
19. Du, Y. K.; Yang, P.; Mou, Z. G.; Hua, N. P.; Jiang, L.; *J. Appl. Polym. Sci.*, **2006**, 99, 23
DOI: [10.1002/app.21886](https://doi.org/10.1002/app.21886)
20. Conway, B. E.; *Electrochemical supercapacitors: scientific fundamentals and technological applications*; Kluwer Academic / Plenum Publishers: USA, **1999**